

# Verification of Coupled Heat and Mass Transfer Model *ISERIT* by Full-scale Experiment

Dalibor Frydrych \* and Milan Hokr \*

**Abstract** — Danger waste disposal systems are typically comprised a series of barriers that act to protect the environment and human health. The presence of several barriers enhances confidence that the waste will be adequately contained. This article is focused on one of barriers, bentonite buffer. Bentonite buffer intervene between the waste canister and the host rock. One of main tasks of the bentonite buffer is to prevent the contact of the underground water from host rock with the waste canister, for as long time as possible. Model, described in this article, solve coupled task of unsteady heat and water vapor flow in bentonite. In the end, model results are compared with results obtained from full-scale experimental site.

**Keywords:** *modelling, coupled problem, heat and mass*

## 1 Introduction

The major problem of dangerous (radioactive or toxic) waste repositories is water present in the host rock. The water does not only jeopardize the integrity of the waste canister, but also, form possible pathway to the biosphere, if the hazardous substances leak out of waste canister.

The problem of re-saturation of the initially air-dry bentonite is very complex [4]. This phenomenon is influenced by hydraulic, mechanic, thermal and chemical processes. These processes are coupled by a series of parameters and equations. Some of them are highly nonlinear and some of them are not yet completely understood.

For better understanding of this complicated processes an in order to verify the precision of models, several experiments were prepared a realized. Comparing of results obtained from model with results received by experiments gave the opportunity for gradual improvements in models, to bring them to the expected level. Experimental devices had different sizes, from small laboratory instruments up to full-scale devices installed in-situ. Obviously in-situ experiments were the most difficult.

Model *ISERIT* described in this article, will be compared with results of one of full-scale in-situ experiment.

### 1.1 Full-scale experiment

The experiment known as "Buffer/Container Experiment" [2] was realized by *Atomic Energy of Canada Limited* in the *Underground Research Laboratory, Lac du Bonnet, MB*. Experimental site was situated in room excavated at 240 m depth. All dimensions were the same, as conceptual design of the reference vault, borehole had diameter 1.24 m and depth 5 m, container had diameter 0.635 m and was 2.25 m tall, see figure 1. Container was surrounded by 5 cm layer of quartz sand. Rest of volume of the vault was filled in by compacted bentonite buffer. The sand layer, bentonite buffer and rock was instrumented with a series of thermistors, psychrometers, packer strings, pressure transducers, displacement gauges and radial strain cells to monitor how the were affected by the heater. Content of container was replaced by electric heater. Heater simulated disintegration heat of the waste, 1000 W in first 26 days and 1200 W to the end of experiment. Total time of experiment was 896 days.

The host rock contains water with potential well in excess of atmospheric pressure, while the water in unsaturated buffer had much lower potentials corresponding to suction pressures lower than atmospheric pressure. Under these conditions, water was moved towards the heater down the hydraulic gradient from the rock into the buffer. Immediately after the heater was switched on, a number of coupled processes were started. Heat was flowed through the buffer towards the cooler rock, causing temperatures to rise. Water which was initially uniformly distributed throughout the buffer was migrated down the temperature gradient away from the heater towards the buffer-rock interface.

Many scientists have worked with models, solved this problem using Darcy law. But these type of models do not reflect effect of water vapor generated by heat from nuclear waste or, as it was in the experiment, by electric heater.

In this article is presented model, which solve this task in

\*Technical University of Liberec, Faculty of Mechatronics and Interdisciplinary Engineering Studies, Institute of new technologies and applied informatics, Studentská 2, 461 17 Liberec, CZECH REPUBLIC, EUROPE, Emails: ffast\_train@quick.cz, milan@seznam.cz

a specific way. This model is based on water vapor diffusion [4]. Model *ISERIT* was designed on TU of Liberec. Model *ISERIT* solve the unsteady coupled heat and moisture transfer problem in porous materials with sorption of moisture in solid phase by using primal formulation of finite element method.

$$\begin{aligned}
 c_v(T, C_a, C_b) \frac{\partial T}{\partial t} - \chi(T, C_a, C_b) \frac{\partial C_b}{\partial t} &= \nabla \cdot (\lambda(T, C_a, C_b) \nabla T) \quad , \\
 \epsilon \frac{\partial C_a}{\partial t} + (1 - \epsilon) \frac{\partial C_b}{\partial t} &= \nabla \cdot \left( \frac{\epsilon}{\tau} D_a(T, C_a, C_b) \nabla C_a \right) \quad , \\
 \frac{1}{\epsilon} \frac{\partial C_b}{\partial t} &= \left( \frac{C_a}{C_a^{100}(T)} - \varphi(T, C_a, C_b) \right) \gamma(T, C_a, C_b) \quad .
 \end{aligned}
 \tag{1}$$

Domain of task is denoted  $\Omega$  with boundary  $\Gamma$ . The problem is discreted in the space variable  $\mathbf{x} = \{x, y\}$ .

Unknown variables are  $T$  temperature,  $C_a$  water vapor concentration in the air between bentonite grains and  $C_b$  water vapor concentration in the bentonite grains.

Furthermore  $t$  time,  $c_v(T, C_a, C_b)$  volumetric heat capacity,  $\chi(T, C_a, C_b)$  latent heat of sorption or adsorption of water vapor by solid grains (it gives information on interaction forces between the water vapor molecules and the sorbent surface-binding energy),  $\lambda(T, C_a, C_b)$  thermal conductivity,  $\epsilon$  porosity of bentonite,  $\tau$  effective tortuosity (it is related to the hindrance imposed on diffusing particle by the bentonite grains),  $D_a(T, C_a, C_b)$  diffusion coefficient of water vapor in the air,  $C_a^{100}(T)$  water vapor concentration for 100% relative humidity (RH) in the air,  $\varphi(T, C_a, C_b)$  inversion sorption curve, and  $\gamma = \gamma(T, C_a, C_b)$  general function defining sorption/adsorption speed of bentonite.

Material parameter  $c_v$ ,  $\chi$ ,  $\lambda$ ,  $D_a$ ,  $C_a^{100}$ ,  $\gamma$  and  $\varphi$  are assumed as functions and must be positive and limited.

### 2.1 Boundary conditions

The set of boundary conditions is added. In the model are assumed three kinds of boundary conditions. Splitting of boundary  $\Gamma$  on three disjunction parts  $\Gamma = \Gamma_1 \cup \Gamma_2 \cup \Gamma_3$  is assumed.  $\mathbf{n}$  is outer normal of boundary  $\Gamma$ .

**Dirichlet boundary condition** defined temperature  $T_D(t)$ , eventually water vapor concentration  $C_D^a(t)$  on boundary  $\Gamma_1$ ,

$$\begin{aligned}
 T(\mathbf{x}, t) &= T_D(t) \\
 C_a(\mathbf{x}, t) &= C_D^a(t) \quad \mathbf{x} \in \Gamma_1 \quad .
 \end{aligned}
 \tag{2}$$

## 2 Problem formulation

Heat and mass transportation parameters and the distribution of moisture and temperature within porous materials are based on the energy and moisture conservation equations during the transportation. The transfer is described by partial differential equations derived from the set of equations (1) published by Henry [3]

**Neumann boundary condition** defined heat flow  $q_T(t)$ , eventually water vapor flow  $q_{C_a}(t)$  through boundary  $\Gamma_2$ ,

$$\begin{aligned}
 \lambda \nabla T(\mathbf{x}, t) \cdot \mathbf{n} &= q_T(t) \\
 D_a \nabla C_a(\mathbf{x}, t) \cdot \mathbf{n} &= q_{C_a}(t) \quad \mathbf{x} \in \Gamma_2 \quad .
 \end{aligned}
 \tag{3}$$

**Newton boundary condition** defined heat flow, eventually water vapor flow generated by heat drop  $T - T_W(t)$ , eventually by water vapor concentration drop  $C_a - C_W^a(t)$  on boundary  $\Gamma_3$ ,

$$\begin{aligned}
 \lambda \nabla T \cdot \mathbf{n} + \sigma_T(t)(T - T_W(t)) &= 0 \\
 D_a \nabla C_a \cdot \mathbf{n} + \sigma_{C_a}(t)(C_a - C_W^a(t)) &= 0 \quad \mathbf{x} \in \Gamma_3 \quad ,
 \end{aligned}
 \tag{4}$$

where  $\sigma_T(t) > 0$  and  $\sigma_{C_a}(t) > 0$ .

### 2.2 Initial conditions

Initial conditions are defined by general functions on domain  $\Omega$ . These functions can be known, for example constant functions, or can be obtained by solutions of steady task.

$$\begin{aligned}
 T(\mathbf{x}, 0) &= T_o(\mathbf{x}) \\
 C_a(\mathbf{x}, 0) &= C_o^a(\mathbf{x}) \\
 C_b(\mathbf{x}, 0) &= C_o^b(\mathbf{x}) \quad \mathbf{x} \in \Omega \quad .
 \end{aligned}
 \tag{5}$$

### 2.3 Weak formulation

To use the finite element method, the weak formulation has to be derived. Let be  $H_0(\Omega) = \{f \in W_2^1(\Omega), f|_{\Gamma} = 0\}$  the space of testing functions. Further are denoted the scalar products as  $(\varphi, \psi) = \int_{\Omega} \varphi \psi d\Omega$ ,  $\langle \varphi, \psi \rangle = \int_{\Gamma} \varphi \psi d\Gamma$ . Equations in set of equations (1) are multiplied by testing function  $w \in H_0(\Omega)$  and integrated over  $\Omega$ . Then a Green formula is used and substitution of boundary conditions gives integral identities

$$\begin{aligned} \left( c_v \frac{\partial T}{\partial t}, w \right) - \left( \chi \frac{\partial C_b}{\partial t}, w \right) &= \left\langle \lambda \nabla T \cdot \mathbf{n}, w \right\rangle - (\lambda \nabla T, \nabla w), \\ \left( \epsilon \frac{\partial C_a}{\partial t}, w \right) + \left( (1 - \epsilon) \frac{\partial C_b}{\partial t}, w \right) &= \left\langle \frac{\epsilon}{\tau} D_a \nabla C_a \cdot \mathbf{n}, w \right\rangle - \left( \frac{\epsilon}{\tau} D_a \nabla C_a, \nabla w \right), \\ \left( \frac{1}{\epsilon} \frac{\partial C_b}{\partial t}, w \right) &= \left( \gamma \frac{C_a}{C_a^{100}}, w \right) - (\gamma \varphi, w). \end{aligned} \tag{6}$$

The problem is solved in time interval  $I = \langle 0, t^* \rangle$ . Then  $T^*, C_a^*, C_b^* \in AC(I, W_2^1(\Omega))$  is denoted as the function fulfilling the Dirichlet boundary conditions (2). Let

$$\begin{aligned} T(x, t) &= T^*(x, t) + T_0(x, t), \\ C_a(x, t) &= C_a^*(x, t) + C_{a0}(x, t), \\ C_b(x, t) &= C_b^*(x, t) + C_{b0}(x, t), \end{aligned}$$

where  $T_0, C_{a0}, C_{b0} \in AC(I, H_0(\Omega))$ . Then functions  $T, C_a, C_b$  are the weak solution of set of equations (1) with boundary conditions (2)-(4) and initial conditions (5) in time interval  $I$ , if they fulfill the identities (6) for arbitrary  $w \in H_0(\Omega)$ .

Existence of integrals in (6) is allowed by the limit of functions  $c_v, \chi, \lambda, D_a, C_a^{100}, \gamma$  and  $\varphi$ .

## 2.4 Spatial discretization

For spatial discretization the elements (tetrahedrons) with linear base functions are used. Domain of task  $\Omega$  is then approximated by the set  $\Omega^h$ ,

$$\Omega^h = \bigcup_{e \in E^h} e,$$

$$\begin{pmatrix} \mathbb{B}_T & 0 & \mathbb{C}_T \\ 0 & \mathbb{B}_{C_a} & \mathbb{C}_{C_a} \\ 0 & 0 & \mathbb{B}_{C_b} \end{pmatrix} \frac{d}{dt} \begin{pmatrix} T \\ C_a \\ C_b \end{pmatrix} + \begin{pmatrix} \mathbb{A}_T & 0 & 0 \\ 0 & \mathbb{A}_{C_a} & 0 \\ 0 & \mathbb{C}_{C_b} & \mathbb{A}_{C_b} \end{pmatrix} \begin{pmatrix} T \\ C_a \\ C_b \end{pmatrix} = \begin{pmatrix} R_T \\ R_{C_a} \\ R_{C_b} \end{pmatrix}, \tag{8}$$

Items in equation (8) represent

$$\begin{aligned} [\mathbb{A}_T]_{i,j} &= \lambda (\nabla w_i, \nabla w_j), \\ [\mathbb{A}_{C_a}]_{i,j} &= \frac{D_a \epsilon}{\tau} (\nabla w_i, \nabla w_j), \\ [\mathbb{A}_{C_b}]_{i,j} &= \gamma \varphi(w_i, w_j), \end{aligned}$$

$$\begin{aligned} [\mathbb{B}_T]_{i,j} &= c_v(w_i, w_j), \\ [\mathbb{B}_{C_a}]_{i,j} &= \epsilon(w_i, w_j), \\ [\mathbb{B}_{C_b}]_{i,j} &= \frac{1}{\epsilon}(w_i, w_j), \end{aligned}$$

$$\begin{aligned} [\mathbb{C}_T]_{i,j} &= \chi(w_i, w_j), \\ [\mathbb{C}_{C_a}]_{i,j} &= (1 - \epsilon)(w_i, w_j), \\ [\mathbb{C}_{C_b}]_{i,j} &= -\frac{\gamma}{C_a^{100}}(w_i, w_j), \end{aligned}$$

where  $E^h$  is the set of all discretization elements. On every element  $e$  with nodes  $(n^1, n^2, n^3, n^4)$ , four base functions are established,

$$w_i = \alpha_1^i + \alpha_2^i x_2 + \alpha_3^i x_3 + \alpha_4^i x_4, \quad i = 1, 2, 3, 4.$$

They fulfill the condition  $w_i(s^j) = \delta_{ij}$ . The approximation of weak solution is looked for in the form ( $r$  is number of nodes)

$$\begin{aligned} T^h(\mathbf{x}, t) &= \sum_{i=1}^r T^i(t) w_i(\mathbf{x}), \\ C_a^h(\mathbf{x}, t) &= \sum_{i=1}^r C_a^i(t) w_i(\mathbf{x}), \\ C_b^h(\mathbf{x}, t) &= \sum_{i=1}^r C_b^i(t) w_i(\mathbf{x}). \end{aligned} \tag{7}$$

Coefficients  $T^i(t), C_a^i(t), C_b^i(t)$  are values of unknowns at the nodes of discretization in time  $t$ . The approximations (7) are entered into identities (6). Then is searched for their fulfillment for all base functions  $w_j, j \in \hat{r}$ . The resulting system of ordinary differential equations has the block structure, see equation (8).

$$\begin{aligned} [R_T]_i &= \lambda \langle \alpha, w_i \rangle, \\ [R_{C_a}]_i &= \frac{D_a \epsilon}{\tau} \langle \beta, w_i \rangle, \\ [R_{C_b}]_i &= 0, \end{aligned}$$

$$\begin{aligned} [T]_i &= T^i(t), \\ [C_a]_i &= C_a^i(t), \\ [C_b]_i &= C_b^i(t). \end{aligned}$$

Values of functions  $c_v, \chi, \lambda, D_a, C_a^{100}, \gamma$  and  $\varphi$  in given time are chosen to be piecewise constant on each element (in the manner described further). Values of functions  $\epsilon$  and  $\tau$  are also chosen to be piecewise constant on each element, but as material characteristic, independent on time.

### 3 Numerical model

System (8) with initial conditions (5) can be solved e.g. by the Euler method. Its advantage is, that it can be used for case, when the system has coefficients depending on unknown quantities ( $c_v, \chi, \lambda, D_a, C_a^{100}, \gamma$  and  $\varphi$ ).

#### 3.1 Time discretization

The implicit scheme for approximation of time derivatives is used,

$$\left. \frac{\partial f}{\partial t} \right|_{t=n} \equiv \frac{f^{n+1} - f^n}{\Delta t} .$$

This scheme provides sufficient numerical stability. Then the system (8) can be rewritten more simply,

$$\mathbb{D}\dot{X} + \tilde{\mathbb{D}}X = R ,$$

where

$$\mathbb{D} = \begin{pmatrix} \mathbb{B}_T & 0 & \mathbb{C}_T \\ 0 & \mathbb{B}_{C_a} & \mathbb{C}_{C_a} \\ 0 & 0 & \mathbb{B}_{C_b} \end{pmatrix} ,$$

$$\tilde{\mathbb{D}} = \begin{pmatrix} \mathbb{A}_T & 0 & 0 \\ 0 & \mathbb{A}_{C_a} & 0 \\ 0 & \mathbb{C}_{C_b} & \mathbb{A}_{C_b} \end{pmatrix} ,$$

$$X = \begin{pmatrix} T \\ C_a \\ C_b \end{pmatrix} , \quad R = \begin{pmatrix} R_T \\ R_{C_a} \\ 0 \end{pmatrix} .$$

$$\begin{pmatrix} \mathbb{B}_T + \Delta t \mathbb{A}_T^{(n)} & 0 & \mathbb{C}_T \\ 0 & \mathbb{B}_{C_a} + \Delta t \mathbb{A}_{C_a}^{(n)} & \mathbb{C}_{C_a} \\ 0 & \Delta t \mathbb{C}_{C_b}^{(n)} & \mathbb{B}_{C_b} + \Delta t \mathbb{A}_{C_b}^{(n)} \end{pmatrix} \begin{pmatrix} T^{(n+1)} \\ C_a^{(n+1)} \\ C_b^{(n+1)} \end{pmatrix} = \tilde{R}^{(n)} . \quad (9)$$

### 4 Model ISERIT

Implementation of numerical model defined in chapter 3 was named *ISERIT*. Model *ISERIT* is based on Methodology *DF<sup>2</sup>EM* [1]. Implementation of model *ISERIT* consisted only of creation 24 classes (are divided into 6 packages), 12 classes out of 24 classes realized boundary conditions. Implementation of model *ISERIT* took approximately 3 weeks.

#### 4.1 Model of experimental site

Design of experimental site and material parameters was published in [2]. In order to simplify calculations and for better orientation, new zero point of coordinate system was defined. The zero point is placed at intersection of containers axis and plane of the access room floor.

First step in creation of experimental site model was the definition of model boundary. If the boundary was cho-

Values  $D_a, K, \gamma$  in  $n^{th}$  time step were implicitly chosen by substituting the guess  $\hat{X}^{(n+1)}$  in time step  $(n+1)$ . Matrix  $\tilde{\mathbb{D}}$  and right hand side  $R$  are time-dependent, more accurately, they depend on values  $c_v, \chi, \lambda, D_a, C_a^{100}, \gamma$  and  $\varphi$  which consist in  $X$ . For  $n^{th}$  time step, they are having form

$$\tilde{\mathbb{D}}^{(n)} = \tilde{\mathbb{D}}(\hat{X}^{(n+1)}) , \quad R^{(n)} = R(\hat{X}^{(n+1)}) .$$

Consequently, the problem

$$\mathbb{D} \frac{X^{(n+1)} - X^{(n)}}{\Delta t} + \tilde{\mathbb{D}}^{(n)} X^{(n+1)} = R^{(n)} ,$$

was solved and the variation between the solution  $X^{(n+1)}$  and the guess  $\hat{X}^{(n+1)}$  was watched. For the large variation, the solution  $X^{(n+1)}$  was used as new estimate  $\hat{X}^{(n+1)}$  (for first iteration we used  $\hat{X}^{(n+1)} \equiv X^{(n)}$ ). This process was repeated several times until only small variation are reached. Then the new initial problem for time step  $(n+2)$  was solved. In particular iteration in  $n^{th}$  time step the linear system is solved,

$$(\mathbb{D} + \Delta t \tilde{\mathbb{D}}^{(n)}) X^{(n+1)} = R^{(n)} \Delta t + \mathbb{D} X^{(n)} .$$

If denoted

$$R^{(n)} \Delta t + \mathbb{D} X^{(n)} = \tilde{R}^{(n)} ,$$

the linear system can be written in block structure,

sen too near, boundary conditions (BC) defined on this boundary would have negative influence on model results. In the experiment, the most remote sensors were placed 12 m from container axis and recorded only minimal changes of the measured parameters. Taking to account this finding, the model boundaries were put 15 m from the zero point.

Discretization of model area (mesh generation) was complicated process. It was necessary to take into account five centimeter sand layer between container and bentonite buffer. This layer has the lowest thermal conductivity from all materials in this area. Consequently, there will be the highest temperature gradient in this area. It was therefore necessary that the layer is defined in the model by at least two layers of elements. However, such a fine discretization of the whole area would mean too high number of nodes and elements. That would lead to too high number of linear equations needed for the calculations. This problem was solved by the following:

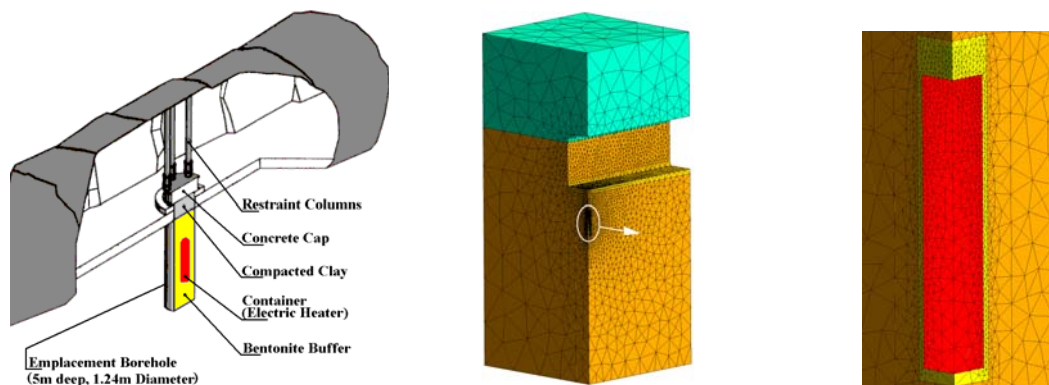


Figure 1: Cutaway View of the Buffer/Container Experiment (left); Main view on model mesh of experimental site (center); Detail view on model mesh of container and buffer (right)

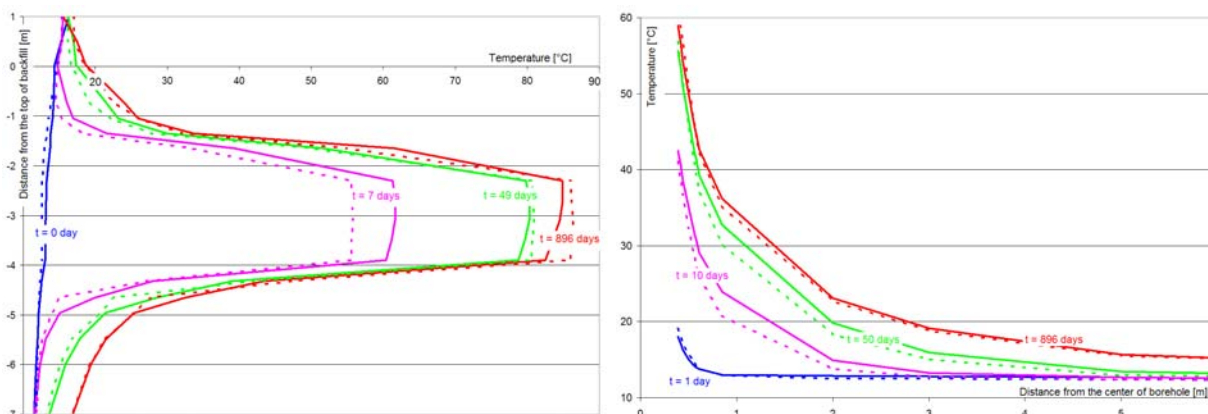


Figure 2: Evolution of temperature; vertical profiles (left), horizontal profiles (right) (continuous line - experimental data, dashed line - data computed by model)

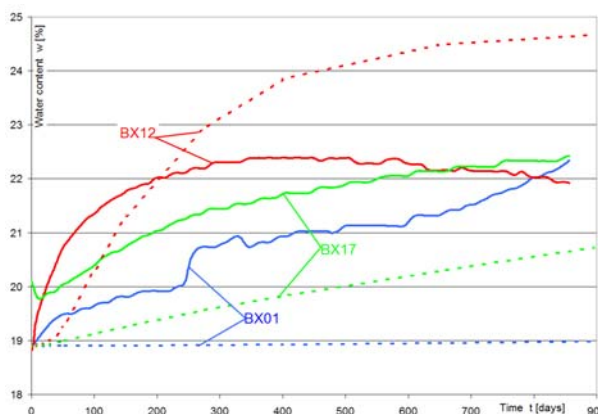


Figure 3: Evolution of water content in measurement points BX01, BX12 and BX17 (continuous line - experimental data, dashed line - data computed by model)

- By using principle of symmetry, model deals only with one quadrant, see figure 1 (left).
- The mesh is unevenly structured. Elements in sand layers have edges shorter than 2 cm. On the other hand, elements placed on the area boundaries were the temperature gradient is minimal, have edges longer than 2 m, see figure 1 (center and right).

This mesh contains of 13227 nodes and 66758 elements (tetrahedrons).

## 4.2 Model of experiment scenario

Scenario of experiment was published in [2]. Time interval of this scenario is 896 days. In calculation scenario were used time steps of different lengths, 0.5 day up to 250 days.

The initial temperature was calculated as steady task. Temperature was entered on top, back and bottom wall, see figure 1 (center). Temperature on these three walls was given by Dirichlet BC (2), with value  $T = 11^{\circ}\text{C}$ . Room walls were warmed up by current air. Their temperature was given by Newton BC (4), with value  $T = 16^{\circ}\text{C}$  a parameter  $\sigma_T = 50^{\circ}\text{Cm}^{-1}$ . Parameter  $\sigma_T$  is chosen as the best guess and was improved by iterations. On the front and both side walls, see figure 1 (center), was given Neumann BC with value  $q = 0\text{W}$ . This BC is given by principle of symmetry, see section 4.1. These BCs are applied for the complete calculation run.

The initial water content of bentonite buffer was given  $w = 18\%$  (5). The value is the value measured during bentonite buffer installation.

In next steps of calculation scenario was added Neumann BC (3), on the area which represented heater, red part on figure 1 (left). In time interval  $t = (0, 26)$  days, the entered value of BC  $q_1 = 250\text{W}$ . This value corresponds to one quarter of total power of heater  $P_1 = 1000\text{W}$ . In time interval  $t = (26, 896)$  days, the entered value of BC was increased to  $q_2 = 300\text{W}$ . This value corresponds to one quarter of total power of heater  $P_2 = 1200\text{W}$ .

All boundaries of bentonite buffer were closed for water vapors. The Neumann BC (3)  $q = 0\text{gs}^{-1}$  is applied for hole calculation scenario.

## 4.3 Comparison of results

Results obtained by experiment were published in [2]. Model results was compared with experimental results by entering the results into common graphs.

The temperatures in measured points (thermistors) are shown in graphs on figure 2. Graph on left side shows result of measuring points placed on vertical line parallel to heater axis. Graph on right side shows result of measuring points placed on horizontal line perpendicular to heater axis and going through center of the heater. These graphs show very good correlation between temperatures calculated by model and temperatures measured during the experiment. Biggest deviations (around  $5^{\circ}\text{C}$ ) are lo-

calized in the area of sand layer around the heater. In this layer is high temperature gradient and small difference in placing of temperature sensor causes an important deviation. The same deviation can be caused also by material differences or material tamping in this layer.

Results of model concerning of water content simulation are not as good. The water content is measured in several points by psychrometers. These points were placed in defined point in the bentonite buffer. Water content is shown in graph on figure 3. The curves showing real and modeled simulated parameters have different values, but are of similar shapes.

## 5 Conclusion

Model *ISERIT*, described in this article, solve the task of heat transport, with very good accuracy, see figure 2. Task of moisture transport with diffusion in porous media is solved by model *ISERIT* in less precise way, see figure 3.

Model deals only with diffusion of water vapors and does not take in to consideration underground water present in host rock fractures. Therefore, this model itself is not able to fully describe the processes in "real-life" bentonite buffer. In order to get better results, it is necessary integrate this model also equations dealing with water in liquid phase. Such model would then not only took into account influence of underground water, but also water phase changes. This model upgrade is today in an intensive preparation phase.

## Acknowledgements

This work has been supported by Ministry of Education of the Czech Republic; under the project "Advanced remedial technologies and processes", code 1M0554.

## References

- [1] Frydrych, D., Lisal, J., "Introduction to Methodology *DF<sup>2</sup>EM* - Framework for Efficient Development of Finite Element Based Models" *ICCSA '08 - International Conference on Computer Science and Applications*, San Francisco, USA, 10/2008
- [2] Graham, J., *The Buffer/Container Experiment: Results, Synthesis, Issues*, Whiteshell Laboratories, Pinawa, Manitoba, 1997, [online] URL: <<http://collection.nlc-bnc.ca/100/200/301/atomic%5Fenergy%5Fcanada/aecl%5Freports/1997/AECL-11746.pdf>>
- [3] Henry, P.S.H., "Diffusion in Absorbing Media", *Proceedings of the Royal Society of London*, Mathematical and Physical Sciences, Vol. 171, No. 945, pp. 215–241, London, 1939
- [4] Krohn, K. P., *About the role of vapour transport during bentonite resaturation*, GRS report Nr. 222, 2006